Observer-Free Output Feedback Tracking Control for Collaborative Robotics

Moath Alqatamin, *Member, IEEE*, Nazita Taghavi, *Member, IEEE*, Sumit K. Das *Member, IEEE*, Dan O. Popa*, *Senior Member, IEEE*

Abstract— In this paper, an Observer-Free Output Feedback (OF2) tracking controller is formulated for a robotic manipulator, in order to improve performance during humanrobot collaboration. The OF² controller is based on a set of filtered error dynamics that avoids the need for direct speed measurements or observer design. The main advantage of this method is that it is model-free and robust to changes in operating conditions often present in environments where humans and robots work together. Moreover, OF² controller is demonstrably stable, thus safe, and a Lyapunov stability proof is offered using a nominal dynamic model of the robot. Collaborative robots have highly nonlinear and uncertain dynamic models and are ideal candidates for our controller. The controller can be used to not only compensate for the unknown system parameters, but also reject external disturbances, such as human or environmental forces. Tracking performance of our controller has been tested experimentally on the Baxter collaborative robot under different trajectory tracking and impact experiments with and without payload. The results have been compared with the factory built-in and pre-tuned PID controller. Results indicate that our controller shows an order of magnitude improvement in the trajectory tracking performance and a reduction in joint efforts required during learning from demonstration and assembly tasks.

I. INTRODUCTION

In recent years, collaborative robots have been developed for use in industry, education, health care, and daily life [1]. These robots are employed in different applications alongside humans as aids for repetitive and tedious tasks during manufacturing [2], and also during interaction with social and rehabilitation robots in healthcare [3]. An important requirement for these collaborations is the safety of both the robot and the human user during physical interaction [4]. Furthermore, collaborative robots often need to execute programmed actions with high level of tracking performance, high speed, and accuracy regardless of possible undesirable disturbances from humans and the environment.

A well-known example is the teach by demonstration capability of collaborative robots often used when the robot learns new skills from a human [5]. In this case, both safety and accurate trajectory tracking performances are important during interaction. In our recent work, we developed a human-robot interaction (HRI) algorithm called Adaptive Motion Imitation (AMI) [6]. Using this algorithm, the robotic agent learns a cyclic trajectory performed by a user, and adapts the shape and speed of its motion to follow queues from the human. AMI is sensitive to the shape and speed of the performed trajectory which requires high accuracy for robotic

arm control system regardless of payload carried by the robot. During the implementation of AMI on a robotic testbed in our lab, we noticed that the factory-tuned PID controller of the Baxter does not fulfill tracking requirements especially when the robot needs to carry large loads and move at high speeds.

Another well-known motivating example involves limiting robot impact forces during collisions with humans or the environment. In the realm of safety, different strategies for safe human-robot interaction have been studied in the past decade, leading up to the collaborative robot RIA standard [7]. Many collaborative robot systems utilize costly sensors to detect human presence, for instance tactile, force and vision sensing. For example, [8] developed a rule-based method to resolve the collision issues during the pick and place task performance of a robotic arm. The robot detected objects based on received information from the vision system. [9] considered serial robot manipulators equipped with a dual-type proximity sensor and developed an algorithm based on admittance control to avoid robots from collisions with the obstacle. They also applied a machine learning method to prevent the degradation of the proximity performance Furthermore, most collaborative robots detect joint efforts by monitoring motor currents during operation. However, many robots still lack sensors for human or obstacle detection. In these cases, an approach to maintain safety relies on is control algorithms that limit the impact forces of the robotic arm to a safe and acceptable range. Therefore, if a collision occurs, serious damage can be avoided [10].

For both trajectory tracking and safe operation, numerous model-based control algorithms have been developed for robotic systems, such as compute torque [11], robust control [12], and adaptive control [13]. However, the main disadvantage of these model-based approaches is that their performance degrades due to unknown dynamics and timevarying disturbances. To deal with these challenges, intelligent control techniques such as neural networks (NN) have been incorporated in the controller loops [14, 15]. For instance, neuroadaptive controllers (NAC) have also been envisioned and are entirely model-free, have high tracking performance, and require little calibration of model parameters [16]. In our previous work [17], the NAC was extended to also estimate interaction forces from human operators, a highly variable input. However, a drawback of NN-based robot control methods is the high computational burden that requires high performance computing resources in the feedback loop. For robotic systems with limited computational resources, NNbased controllers are still out of reach. In this paper, an observer-free output feedback torque controller (OF²), based on a set of filtered error signals is designed for a high

^{*} Authors are with Louisville Automation & Robotics Research Institute University of Louisville, KY, USA, email: moath.alqatamin@louisville.edu.

dimensional robotic manipulator with unknown dynamics and external torque disturbance. This controller was originally introduced in [18] for a class of second order systems. A modification has been introduced in this paper by designing an update term to compensate for unmolded and unstructured time varying external disturbances. One advantage of OF² is that it is suitable for the systems with low computational resources. Also, unlike many other methods, OF² controller does not need a speed measurement or observer. The presence of a speed observer usually adds an outer loop to the control scheme which needs to converge faster than the control loop. This means, control loops bandwidth needs to be very fast. Also, performing numerical derivative of the position data to get the speed signal amplifies the encoder measurement noise and leads to a noisy speed signal that need to be filtered out before using it in the control loop. In addition, OF² is modelfree and has both guaranteed tracking and stability performance due to a Lyapunov proof.

For evaluation of OF², experiments have been performed with a dual-arm, 7 degrees of freedom (DOF) Baxter robot available in our lab. Results show that our controller has very good tracking performance in comparison with the factory pretuned PID controller of the Baxter in different operating conditions, such as high motion frequency and payload. We have specially considered cyclic trajectories for teach by demonstration episodes, since our AMI algorithm is based on repeated trajectories created by Fourier series. Further results during pick and place operation also demonstrated that OF² requires less torque, and generates less energetic impacts with the environment, which means it is safer than the PID controller for physical HRI.

The paper is organized as follows: in section II the filter-based control scheme OF² is formulated, and its Lyapunov stability analysis is discussed. The experimental results validating the controller performance are presented and discussed in section III. Finally, the conclusion and the future work are presented in section IV.

II. CONTROLLER FORMULATION AND STABILITY ANALYSIS

The dynamic model of an n degree of freedom (nDOF) robotic arm can be classically written as:

$$M(q)\ddot{q}(t) + V(q,\dot{q})\dot{q} + F(\dot{q}) + G(q) + \tau_d = \tau$$
 (1)

where $q(t), \dot{q}(t), \ddot{q}(t) \in \mathbb{R}^n$ are the joints angular position, velocity and acceleration, respectively [19]. In (1), $M(q) \in \mathbb{R}^{nn}$ is the inertia matrix; $V(q, \dot{q}) \in \mathbb{R}^{nn}$ is the matrix of Coriolis and centrifugal torques; $G(q) \in \mathbb{R}^n$ is the vector of gravitational torques; $F(\dot{q}) \in \mathbb{R}^n$ is the friction vector. $\tau_d(t) \in \mathbb{R}^n$ represents unknown external disturbance torque. $\tau(t) \in \mathbb{R}^n$ is the vector of the input torque that represents the control torque to be designed. One of the well-known structural properties of the robot dynamic equation is listed below:

Property: The inertia matrix M(q) is a positive definite symmetric and lower and upper bounded as

 $m_1 ||\chi||^2 \le \chi^T M(q) \chi \le m_2 ||\chi||^2$, where m_1, m_2 are known positive constants and $||\chi||$ is the Euclidean 2-norm of an arbitrary vector $\chi \in \mathbb{R}^n$.

In addition, the subsequent controller development is based on the following standard assumptions about the robot dynamic equation:

Assumption 1: $M(q), V(q, \dot{q}), F(\dot{q}), G(q)$ are unknown matrices and vectors but bounded and differentiable.

Assumption 2: $\tau_d(t)$ is a slowly time-varying bounded unknown external disturbance torque.

Assumption 3: The desired trajectories $q_d(t)$ are bounded and continuous differentiable.

The objective of the proposed controller is to ensure that the output positions of the robotic arm joints are tracking the desired trajectories $q_q(t) \in \mathcal{L}_{\infty}$ in the presence of unknown system parameters and unknown external disturbance with only the angular position is measurable (output feedback control scheme). Hence, $q(t) \to q_d(t)$ as $t \to \infty$. For this objective, the position tracking error e(t) should be defined as:

$$e \triangleq q_d - q \tag{2}$$

Moreover, in order to compensate for the lack of the velocity measurement, the following filter dynamics is introduced as:

$$\dot{e}_f \triangleq -e_f + r_f \tag{3}$$

$$r_f \triangleq p - (k_2 + 1)e \tag{4}$$

$$\dot{p} \triangleq -r_f - (k_2 + 1)(e + r_f) + e - e_f$$
 (5)

where $e_f(t), r_f(t) \in \mathbb{R}^n$ are the filtered signals, $p(t) \in \mathbb{R}^n$ is an auxiliary variable introduced to write the filter $r_f(t)$ in implementable form. k_2 is a positive constant.

To start the control development, the error signal $\eta(t) \in \mathbb{R}^n$ is defined as:

$$\eta \triangleq \dot{e} + e + r_f \tag{6}$$

By taking the time derivative of (4), and substituting (5), the dynamic filter is obtained:

$$\dot{r}_f = -r_f - (k_2 + 1)\eta + e - e_f \tag{7}$$

After taking the time derivative of (6) and front premultiplying by M(q), the following equation can be obtained:

$$M(q)\dot{\eta} = M(q)\ddot{e} + M(q)\dot{e} + M(q)\dot{r}_f \tag{8}$$

By substituting the second time derivative of (2), the system dynamics from (1), $\dot{r}_f(t)$ from (7) and $\dot{e}(t)$ from (6) into (8), and after some mathematical simplification, the following $\eta(t)$ open-loop error dynamics can be written as:

$$M(q)\dot{\eta} = -k_2 M(q) \eta - M(q) \left(e_f + 2r_f \right)$$

$$+ Y + \tau_d - \tau$$
(9)

where the auxiliary term $Y(q, \dot{q})$ is defined as:

$$Y(q, \dot{q}) = M(q)\ddot{q}_d + V(q, \dot{q})\dot{q} + F(\dot{q}) + G(q)$$
 (10)

By defining $Y_d \triangleq Y(q_d, \dot{q}_d)$ as the desired trajectories of the auxiliary signal $Y(q, \dot{q})$, it is easy to see that Y_d, \dot{Y}_d are bounded based on Assumption 1. Then, the open loop error dynamics can be rewritten as:

$$M(q)\dot{\eta} = -k_2 M(q) \eta - \frac{1}{2} \dot{M}(q) \eta + \tilde{Y} + Y_d + \tau_d - \tau, \tag{11}$$

where $\tilde{Y}(q, \dot{q}, e_f, r_f, \eta)$ is defined as:

$$\tilde{Y} \triangleq Y - Y_d - M(q) \left(e_f + 2r_f \right) + \frac{1}{2} \dot{M}(q) \eta \tag{12}$$

From the open-loop error dynamic of $\eta(t)$ in (9) and motivated by the subsequent stability analysis, the following control torque is designed as:

$$\tau \triangleq K_1 sgn(e + e_f) - (k_2 + 1)r_f + e + \hat{\tau}_d,$$
 (13)

where $K_1 \in \mathbb{R}^{nn}$ is positive control gains matrix which is selected based on the subsequent stability analysis. $sgn(\cdot)$ is the standard signum function. $\hat{\tau}_d(t)$ is the estimation of the external disturbance torque which designed based on the stability analysis to be:

$$\dot{\hat{\tau}}_d \triangleq K_d \eta, \tag{14}$$

where K_d is a positive estimation gain. From (14) it is clear that this update law is not implementable because it has velocity measurement in the definition of $\eta(t)$. By using (6) and making the integration, the following realizable form can be found as:

$$\hat{\tau}_d = K_d[e(t) - e(0) + \int_0^t (e + r_f) d\sigma].$$
 (15)

After substituting (13) into (9), the closed-loop error dynamics for $\eta(t)$ becomes:

$$M(q)\dot{\eta} = -k_2 M(q) \eta - \frac{1}{2} \dot{M}(q) \eta + \tilde{Y} + Y_d$$

$$-K_1 sgn(e + e_f) + (k_2 + 1)r_f - e + \tilde{\tau}_d$$
(16)

Where $\tilde{\tau}_d(t)$ is the estimation error of the external disturbance $\tau_d(t)$ defined as:

$$\tilde{\tau}_d \triangleq \tau_d - \hat{\tau}_d. \tag{17}$$

From the definition of $Y(\cdot)$ in (10) and assumptions 1, and by using the mean value theorem, $\tilde{Y}(\cdot)$ can be upper bounded as:

$$||\tilde{Y}|| \le \rho(||z||)||z||,\tag{18}$$

where $z \triangleq \begin{bmatrix} e^T & e_f^T & r_f^T & \eta^T \end{bmatrix}^T$ and $\rho(||z||)$ is a non-decreasing positive function depends on the ∞ -norm of the system errors. The following Lemmas are introduced to be used in the stability proof of the main theorem presented in this section

Lemma 1: The following auxiliary function $L(t) \in \mathbb{R}$ is defined as:

$$L \triangleq \eta^T \left(Y_d - K_1 sgn(e + e_f) \right). \tag{19}$$

If K_1 is selected to satisfy the following condition:

$$K_{1i} > ||Y_{di}||_{\infty} + ||\dot{Y}_{di}||_{\infty},$$
 (20)

where i = 1, 2, ..., n represents the ith element of the diagonal K_1 matrix. Then,

$$\int_0^t L(\sigma)d\sigma \le \gamma,\tag{21}$$

where γ is a positive constant selected to satisfy the following condition:

$$\gamma \triangleq \sum_{i=1}^{n} K_{1i} |e_i(0)| - e^T(0) Y_d(0). \tag{22}$$

Based on the above, the following positive definite function $P(t) \in \mathbb{R}$ can be defined as:

$$P(t) \triangleq \gamma - \int_0^t L(\tau)d\tau, \tag{23}$$

Proof: See Appendix A in [20].

Lemma 2: Define the region \mathfrak{D} to be as: $\mathfrak{D} \triangleq \{y \in \mathbb{R}^m | ||y|| < \varepsilon \varepsilon \text{ is a positive constant. Also, define } V(t,y): \mathbb{R}^+ \times \mathfrak{D} \to \mathbb{R}^+ \text{ to be a continuously differentiable function such that:}$

 $W_1(y) \le V(t,y) \le W_2(y)$ and $\dot{V}(t,y) \le -W(y)$ (24) $\forall t \ge 0$ and $\forall y \in \mathfrak{D}$, where $W_1(y), W_2(y)$ are continuous positive definite functions and W(y) is a uniformly continuous positive semi-definite function on \mathfrak{D} . If the condition in (24) is met and $y(0) \in \mathfrak{I}$, the following result is concluded as:

$$W(y(t)) \to 0 \text{ as } t \to \infty,$$
 (25)

where the region 3 should be defined as:

$$\mathfrak{J} \triangleq \{ y \in \mathfrak{D} | W_2(y) \le \delta \tag{26}$$

where $\delta < \min_{||y||=\varepsilon} W_1(y)$ is a positive constant.

Proof: See Theorem 8.4 in [21].

Theorem 1 $(OF)^2$: The proposed observer-free, output feedback control law in (13), (14) and (15) ensure that the error signals $e(t), e_f(t), r_f(t), \eta(t)$ are bounded and $e(t), \dot{e}(t) \rightarrow 0$ as $t \rightarrow \infty$ if K_1 is selected to satisfy the condition in (20) and k_2 as in:

$$k_2 = \frac{k_3 + 1}{m_1} \tag{27}$$

where k_3 is a positive constant chosen based on the stability analysis. k_3 is not explicitly appears in the control law in (13).

Proof: A candidate positive definite Lyapunov function $V(t, y) \in \mathbb{R}$ is defined as:

$$V \triangleq \frac{1}{2}e^{T}e + \frac{1}{2}e_{f}^{T}e_{f} + \frac{1}{2}r_{f}^{T}r_{f} + \frac{1}{2}\eta^{T}M\eta + P, \tag{28}$$

where $y = [z^T \sqrt{P}]^T$. The time derivative of (28) is

$$\dot{V} = e^T \dot{e} + e_f^T \dot{e}_f + r_f^T \dot{r}_f + \eta^T M \dot{\eta} + \frac{1}{2} \eta^T \dot{M} \eta + \dot{P}.$$
 (29)

After substituting the error signals from (3), (6) and (7), along with the closed loop error dynamics from (16) and the update law from (14) into (29), the following expression can be obtained after some mathematical simplifications and after using (19):

$$\dot{V} = -e^T e - e_f^T e_f - r_f^T r_f - k_2 \eta^T M(q) \eta + \eta^T \tilde{Y}$$
(30)
After applying property of $M(q)$ into (30), and using (18) and (27), $\dot{V}(t)$ in (30) can be upper bounded as in (31):

$$\dot{V} \le -||z|| + [||\eta||\rho(||z||)||z|| - k_3||\eta||^2] \tag{31}$$

After completing the square of the bracket term, the following term can be obtained:

$$\dot{V} \le -\left(1 - \frac{\rho^2(||z||)}{4k_3}\right) ||z||^2 = -\alpha ||z||^2$$
 (32)

Where α is positive constant. From the above, $\dot{V}(t)$ is negative definite if $k_3 > \frac{1}{4}\rho^2(||z||)$. By utilizing Lemma 2 and from (24) and (32) it is easy to see that $e(t), e_f(t), r_f(t), \eta(t) \in \mathcal{L}_{\infty}$. Then, from (6) we conclude that

 $\dot{e}(t) \in \mathcal{L}_{\infty}$. From (3), (4) and (5), it is clear that $\dot{e}_f(t), r_f(t), p(t)$ and $\dot{p}(t) \in \mathcal{L}_{\infty}$. Using the above results and from (15), we can say that $\hat{\tau}_d(t) \in \mathcal{L}_{\infty}$. Then, using the previous results and from (13), it is concluded that $\tau(t) \in \mathcal{L}_{\infty}$. Again by using Lemma 2 and (32) we can say that $\alpha ||z||^2 \to 0$ as $t \to \infty$. From the definition of z(t) and using (6) we can conclude that $e(t), e_f(t), r_f(t), \eta(t), \dot{e}(t) \to 0$ as $t \to \infty$. Thus, the proof of *Theorem 1* is completed.

III. EXPERIMENTAL RESULTS

In this section, we discuss experimental evaluation of the OF² controller on the Baxter collaborative robot [22] during learning from demonstration and environmental impact tests. The control scheme was implemented using Python programming language. The generated torques are sent to the joints of the right arm of Baxter robot through Robotic Operating System (ROS) running on Ubuntu 16.05 operating system. The joints are denoted s0 and s1 for the shoulder joints, e0 and e1 for the elbow joints, w0, w1 and w2 for the wrist joints as shown in Fig.1a. Both OF² and the native, factory-tuned PID controller of the Baxter are updated at a 1KHz loop rate. The OF² controller gains have been chosen based on the stability analysis gain conditions and by performance observation to be $k_2 = 30$, $K_d = 1$, and $K_1 = diag(0.9,1,1,0.5,0.5,0.5,0.2)$. These values are selected based on the condition in (20) and the definition of the desired auxiliary signal $Y(q_d, \dot{q}_d)$. If we increase the values more, the controller will be more aggressive because the signum function term in the control structure.

The following experiments were performed with the right arm of the Baxter robot in order to evaluate the performance of our controller in comparison to the performance of the Baxter factory pre-tuned PID joint position controller:

- 1- Trajectory tracking, free space motion without payload.
- 2- Trajectory tracking, free space motion with a 1kg payload.
- 3- Impact safety evaluation for teach by demonstration pick and place scenario.
- 4- Demonstrate the robustness of the proposed controller.

In first two experiments, joints were positioned at $q = [0,0,3.14,0.872,0,0]^T$ radians as shown in Fig.1. A sinewave with amplitude $\pi/6$ rad was used as a desired trajectory of the elbow joint e1 in OF² controller in order to perform elbow lift motion. In the position control mode, the desired trajectories were sent directly to the built-in PID controller. The maximum angular velocity of the joint e1 of Baxter robot is 2rad/sec. So, we chose the operating angular velocities to be 1 rad/sec and 2rad/sec. In the second scenario, a 1kg payload is picked up by the end-effector as shown in Fig.1b, and the same elbow lift motion style for both controllers is performed. To quantify the tracking performance of both controllers the total 2-norm error for all arm's joints was calculated as:

$$\sum_{i=1}^{7} \|e_i\|_2, \tag{33}$$
 where i is the joint index, and e_i is tracking error defined in

where i is the joint index, and e_i is tracking error defined in (2). Moreover, in order to evaluate the torque performance for

each controller, the absolute value of average torque for each joint was calculated and then summed up to give the total absolute average torque as:

$$\sum_{i=1}^{7} |avg(\tau_i)| \tag{34}$$

Figure 2 shows the tracking performance results for both controllers in the first scenario at trajectory frequency of the joint e1 motion equal 1rad/sec. Only the results from joints s1, e1 and w1 are plotted here since these joints have the most effect in this kind of the elbow lift motion style. Table I shows the summary of the total 2-norm error that calculated from (33) for both controllers for each frequency. As it can be seen, OF² has better tracking performance at both frequencies. Also, we can see the PID controller performance much worse in the higher rate with total error jumped from 38.1rad to 84.9 rad by changing the rate from 1rad.sec to 2rad/sec. Figure 2 and Table I show the torques for both controllers for these three joints and the total torque that calculated based on (34) for all joints. From the safety point of view, it is clear that the OF² controller has lower total torque than the PID controller and in the same time has better performance. From the table, the maximum total torque of the OF² controller is 15.4 N.m but for the PID controller was 40.9 Nm.

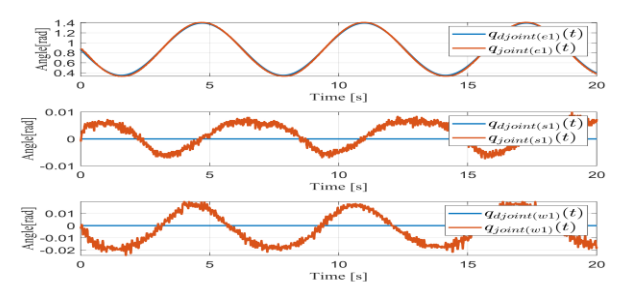


(a)No Payload



(b)With Payload

Figure 1: Baxter robot used in our experiments to validate the performance of our OF² controller.



(a) OF2 Controller

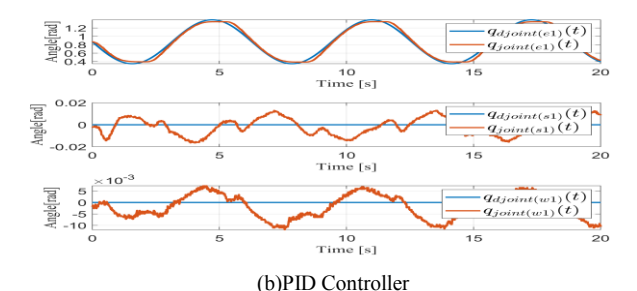


Figure 2: Tracking performance for both controllers without payload and at 1rad/sec speed for joint e1 motion, (a) OF² (b) PID.

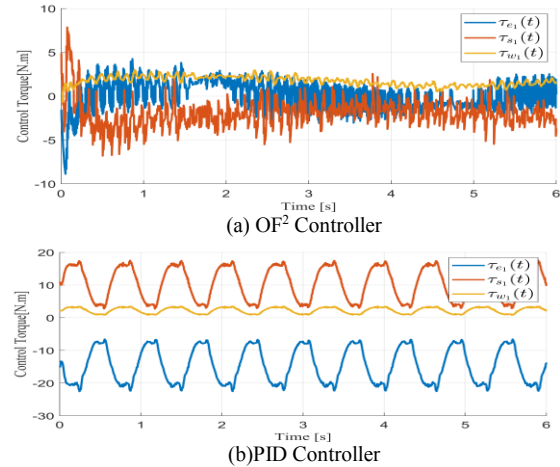


Figure 3: Torque performance for both controllers without payload and at 1rad/sec speed for joint e1 motion, (a) OF² (b) PID/.

In the second experiment, the payload that picked up by the end-effector will change the arm dynamics and increase the inertia of the end-effector. The signum function term in OF² controller in (13) will compensate for this change. In the PID control scheme, usually the gains are tuned for a specific operating conditions. Figure 4 shows the tracking performance of both controllers with payload at 2rad/sec angular frequency of the motion of joint e1. Moreover, Figure 5 shows that the torque of OF² controller is much lower than the torque of the PID controller. Table I further demonstrates and concludes that the performance of OF² control scheme is better than the PID control scheme in terms of tracking performance and the torque that required to perform the motion. Moreover, OF² controller is not using the speed measurement or any kind of observer design.

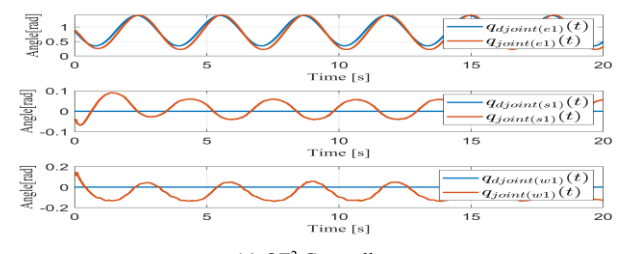
In third experiment, teach by demonstration is performed by the operator to teach the robot arm to mimic a pick and place task of an object placed on a worktable in front of the robot. The goal of this test is to compare the impact performance for both controllers by comparing the torque that required to perform the same task. At the beginning the operator sent a command to enter the teaching mode of Baxter. Then, he grabbed the arm and moved the end-effector to the pick and place location on the worktable. The trajectories of the motion are saved and used as desired trajectories motion for both controllers. The experiments are repeated ten times for each controller. The torque of both controllers are recorded and the total torque based on (34) is calculated for each trial. The average of running ten trials are calculated to be 3.3 N.m and 33.6 N.m for OF² and PID

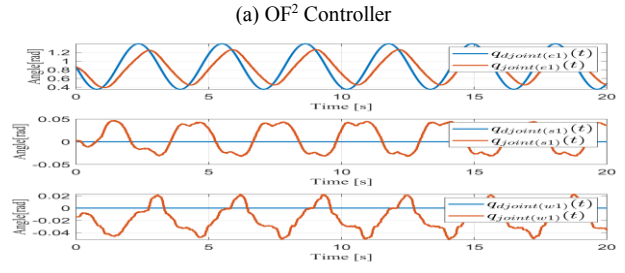
controllers, respectively. It is clear that the torque of OF² controller is significantly lower than the torque of the PID controller, which means it is safer for both human-robot interaction and environmental interaction tasks.

In the fourth experiment, joint s0 is controlled to move to a desired location which in this case was defined by angle $s0=-\pi/6$ rad. Then, an external force was applied to the joint to check the robustness of OF^2 . Figure (6) shows that the proposed OF^2 controller quickly returns the joint to the desired location. For PID controller, it was more difficult to apply the same external force because the joints have very large stiffness due to the high torque. However, both controller rejected average human push disturbances.

Summary of error and torque for both controllers for first two experiments

Speed	Payload	$\sum_{i=1}^{7} e_i _2$		$\sum\nolimits_{i=1}^{7} avg(\tau_i) $	
Rad/sec	kg	PID	OF ²	PID	OF ²
1	0	38.1	29.1	29.3	5.5
2	0	84.9	35.2	30.4	7.6
1	1	39.2	46.7	41.6	13.8
2	1	87.7	58.2	40.9	15.4





(b)PID Controller
Figure 4: Tracking performance for both controllers with payload and at 2rad/sec speed for joint e1 motion, (a) OF² (b) PID.

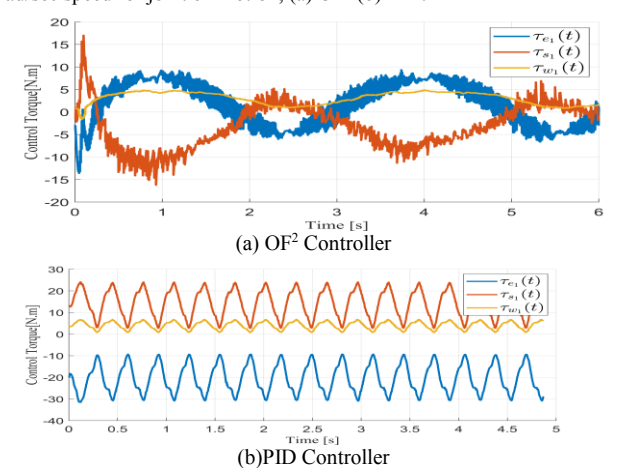


Figure 5: Torque performance for both controllers with payload and at 2rad/sec speed for joint e1 motion, (a) OF² (b) PID.

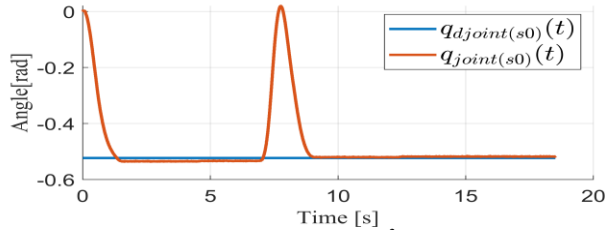


Figure 6: Tracking performance for OF² controller against external disturbance.

IV. CONCLUSION AND FUTURE WORK

In this paper, we formulated OF², a new observer-free, filter-based output feedback controller scheme without the need of speed measurement or observer. Stability and tracking performance guarantees for OF² were derived using a Lyapunov proof. The controller was experimentally evaluated in free motion under cyclic trajectories and also in teach by demonstration assembly scenarios. The results demonstrate that OF² has a better tracking performance than the factory pre-tuned PID controller specifically with high joint rates. Moreover, the results during pick and place operation demonstrated that the OF² control scheme requires 10 x less torque, and therefore generates less energetic impacts with the environment, which means it is safer than the PID controller for physical HRI.

In future work, we will use this controller in parallel with the AMI algorithm for upper body teach by demonstration and adaptive imitation applications.

ACKNOWLEDGMENT

This work was supported by the US National Science Foundation through grants SCH IIS#1838808 and EPSCoR OIA#1849213.

REFERENCES

- [1] R. Luo, C. Huang, Y. Peng, B. Song, and R. Liu, "Repairing Human Trust by Promptly Correcting Robot Mistakes with An Attention Transfer Model," in 2021 IEEE 17th International Conference on Automation Science and Engineering (CASE), 23-27 Aug. 2021 2021, pp. 1928-1933, doi: 10.1109/CASE49439.2021.9551502.
- [2] S. Proia, R. Carli, G. Cavone, and M. Dotoli, "A Literature Review on Control Techniques for Collaborative Robotics in Industrial Applications," in 2021 IEEE 17th International Conference on Automation Science and Engineering (CASE), 23-27 Aug. 2021 2021, pp. 591-596, doi: 10.1109/CASE49439.2021.9551600.
- [3] N. Taghavi, J. Berdichevsky, N. Balakrishnan, K. C. Welch, S. K. Das, and D. O. Popa, "Online Dynamic Time Warping Algorithm for Human-Robot Imitation," in 2021 IEEE International Conference on Robotics and Automation (ICRA), 30 May-5 June 2021 2021, pp. 3843-3849, doi: 10.1109/ICRA48506.2021.9562110.
- [4] I. Ranatunga, S. Cremer, F. L. Lewis, and D. O. Popa, "Neuroadaptive control for safe robots in human environments: A case study," in 2015 IEEE International Conference on Automation Science and Engineering (CASE), 24-28 Aug. 2015 2015, pp. 322-327, doi: 10.1109/CoASE.2015.7294099.
- [5] H. Su, A. Mariani, S. E. Ovur, A. Menciassi, G. Ferrigno, and E. D. Momi, "Toward Teaching by Demonstration for Robot-Assisted Minimally Invasive Surgery," *IEEE Transactions on Automation Science and Engineering*, vol. 18, no. 2, pp. 484-494, 2021, doi: 10.1109/TASE.2020.3045655.

- [6] N. Taghavi, Alqatamin, M. H., and Popa, D.O, "AMI: Adaptive Motion Imitation Algorithm Based on Deep Reinforcement Learning," presented at the IEEE International Conference on Robotics and Automation, PA,USA, MAY, 2022, 2022.
- [7] P. Davison, "Safety Standards and Collaborative Robots."
- [8] I. Lipovanu and C. Pascal, "A rule-based enhancement of a vision guided, collision-free robotic application," in 2021 25th International Conference on System Theory, Control and Computing (ICSTCC), 20-23 Oct. 2021 2021, pp. 559-563, doi: 10.1109/ICSTCC52150.2021.9607077.
- [9] S. J. Moon, J. Kim, H. Yim, Y. Kim, and H. R. Choi, "Real-Time Obstacle Avoidance Using Dual-Type Proximity Sensor for Safe Human-Robot Interaction," *IEEE Robotics and Automation Letters*, vol. 6, no. 4, pp. 8021-8028, 2021, doi: 10.1109/LRA.2021.3102318.
- [10] A. Zacharaki, I. Kostavelis, A. Gasteratos, and I. Dokas, "Safety bounds in human robot interaction: A survey," Safety Science, vol. 127, p. 104667, 2020/07/01/ 2020, doi: https://doi.org/10.1016/j.ssci.2020.104667.
- [11] H. Davis and W. Book, "Torque control of a redundantly actuated passive manipulator," in *Proceedings of the 1997 American Control Conference (Cat. No.97CH36041)*, 6-6 June 1997 1997, vol. 2, pp. 959-963 vol.2, doi: 10.1109/ACC.1997.609669.
- [12] D. Elleuch and T. Damak, "Robust Model-Free Control for Robot Manipulator under Actuator Dynamics," *Mathematical Problems in Engineering*, vol. 2020, p. 7417314, 2020/08/03 2020, doi: 10.1155/2020/7417314.
- [13] Q. Chen, S. Xie, M. Sun, and X. He, "Adaptive Nonsingular Fixed-Time Attitude Stabilization of Uncertain Spacecraft," *IEEE Transactions on Aerospace and Electronic Systems*, vol. 54, no. 6, pp. 2937-2950, 2018, doi: 10.1109/TAES.2018.2832998.
- [14] W. He, A. O. David, Z. Yin, and C. Sun, "Neural Network Control of a Robotic Manipulator With Input Deadzone and Output Constraint," *IEEE Transactions on Systems, Man, and Cybernetics: Systems*, vol. 46, no. 6, pp. 759-770, 2016, doi: 10.1109/TSMC.2015.2466194.
- [15] D. Li and D. Li, "Adaptive Neural Tracking Control for an Uncertain State Constrained Robotic Manipulator With Unknown Time-Varying Delays," *IEEE Transactions on Systems, Man, and Cybernetics:* Systems, vol. 48, no. 12, pp. 2219-2228, 2018, doi: 10.1109/TSMC.2017.2703921.
- [16] F. L. Lewis, "Neural network control of robot manipulators," *IEEE Expert*, vol. 11, no. 3, pp. 64-75, 1996, doi: 10.1109/64.506755.
- [17] S. Cremer, S. K. Das, I. B. Wijayasinghe, D. O. Popa, and F. L. Lewis, "Model-Free Online Neuroadaptive Controller With Intent Estimation for Physical Human–Robot Interaction," *IEEE Transactions on Robotics*, vol. 36, no. 1, pp. 240-253, 2020, doi: 10.1109/TRO.2019.2946721.
- [18] B. Xian, M. S. de Queiroz, D. M. Dawson, and M. L. McIntyre, "A discontinuous output feedback controller and velocity observer for nonlinear mechanical systems," *Automatica*, vol. 40, no. 4, pp. 695-700, 2004/04/01/ 2004, doi: https://doi.org/10.1016/j.automatica.2003.12.007.
- [19] A. Behal, Dixon, W., Xian, B., & Dawson, D.M, Lyapunov-Based Control of Robotic Systems. Boca Raton: CRC Press, 2010.
- [20] B. Xian, D. M. Dawson, M. S. d. Queiroz, and J. Chen, "A continuous asymptotic tracking control strategy for uncertain nonlinear systems," *IEEE Transactions on Automatic Control*, vol. 49, no. 7, pp. 1206– 1211, 2004, doi: 10.1109/TAC.2004.831148.
- [21] H. K. Khalil, *Nonlinear systems*. Upper Saddle, New Jersey: Prentice Hall (in English), 2002.
- [22] S. Cremer, L. Mastromoro, and D. O. Popa, "On the performance of the Baxter research robot," presented at the 2016 IEEE International Symposium on Assembly and Manufacturing (ISAM), Fort Worth, TX, USA, 2016.